

## Resolving Electron Transfer Kinetics at the Nanocrystal/Solution Interface

Peter Liljeroth<sup>†</sup> and Bernadette M. Quinn<sup>‡,\*</sup>

*Condensed Matter and Interfaces, Debye Institute, University of Utrecht, PO Box 80000, 3508 TA Utrecht, The Netherlands, and Laboratory of Physical Chemistry and Electrochemistry, Helsinki University of Technology, PO Box 6100, FIN-02015 HUT, Finland*

Received November 2, 2005; E-mail: bquinn@iki.fi

Controlling the rate of charge transfer through molecular films is of both fundamental and technological interest with relevance to areas such as sensor design and molecular electronics.<sup>1</sup> While electron transfer (ET) kinetics across self-assembled monolayers (SAMs) formed on macroscopic gold surfaces have been studied in depth,<sup>2</sup> relatively little is known about ET across their nanoscale counterpart, SAMs formed on nanoparticle surfaces.<sup>3</sup> The interest in such systems is 2-fold; first, how does the monolayer molecular orientation on the highly curved surface of the nanocrystal (NC) affect the ET process.<sup>3</sup> Second, in small systems, effects such as single-electron charging are expected to have a profound influence on the electrochemical kinetics at the NC “nanoelectrode”.<sup>3,4</sup>

Here, a monolayer of alkanethiolate protected gold nanocrystals (NCs) is used as a model system to investigate ET kinetics between a solution redox mediator and the NC core. Langmuir techniques enable us to tune the interaction between the NCs and thus to change the response between an array of individual nanoelectrodes (weak coupling) to that of an essentially continuous 2D film (strong coupling).<sup>5</sup> This allows us to differentiate between the effects of SAM molecular orientation and the charging of the NCs on the rate of ET. We report the first quantitative estimate for the rate of ET at the nanocrystal/solution interface.

The experimental setup is schematically illustrated in Figure 1. The experimental conditions and particle synthesis have been described in detail elsewhere (ref 6 and Supporting Information). Briefly, known concentrations of monodisperse dodecanethiol protected gold NCs with a core diameter of  $6.6 \pm 0.8$  nm were spread at the air–water interface, and monolayers were transferred at a controlled surface pressure by Langmuir–Schaeffer deposition onto a silanized glass slide. The relevant parameter controlling the coupling between the NCs is the normalized interparticle separation  $d/2a$ , where  $d$  is the center-to-center distance between adjacent NCs and  $a$  is the core radius.<sup>5</sup> The transfer surface pressure ( $\Pi$ ) determines the interparticle separation  $d$  and two films transferred at the extremes of  $d$ , where the film can be considered either as an insulator ( $\Pi = 3$  mN m<sup>-1</sup>,  $d/2a = 1.38$ ) or as a metal ( $\Pi = 20$  mN m<sup>-1</sup>,  $d/2a = 1.19$ ), were used for the ET experiments.<sup>6</sup> Both films consist of close-packed NCs with significant alkanethiol chain interdigitation between neighboring NCs. Scanning electrochemical microscopy (SECM) was used to extract the kinetic parameters. Measurements were performed with a commercially available instrument (CH Instruments, Austin, TX). The SECM tip was biased at a potential in the diffusion-limited region for the oxidation of a solution redox mediator, hexacyanoferrate, and approach curves were recorded where the tip current  $I_L$  is monitored as a function of the distance  $l$  to the NC film. The local depletion of the redox mediator sets up an electrochemical potential gradient in the NC monolayer that causes electron transport to take place (Figure 1).

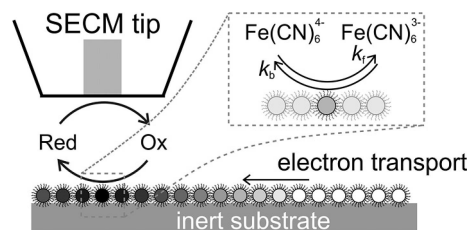


**Figure 1.** Schematic illustration of the experimental setup. The SECM tip was a 25  $\mu\text{m}$  Pt disk microelectrode, and a silver wire served as both counter and reference electrode. The measurements were carried out with  $\text{Fe}(\text{CN})_6^{4-}$  as the redox mediator and 0.1 M  $\text{LiCl}(\text{aq})$  as the base electrolyte.

The electrons are injected into the film by the same redox couple outside the tip–substrate gap. As the film is deposited on an inert substrate, the SECM response is due solely to the properties of the film and not the underlying substrate.

The rate of ET between the metal NCs and the solution redox mediator is governed by the driving force (electrochemical potential of the electrons in the NC monolayer), the electric conductivity of the monolayer, and the kinetics of ET.<sup>6</sup> The well-defined geometry of the SECM allows *quantitative* modeling of the mass-transport, and the model accounts for both mass transport of the solution redox couple and charge transport in the film. The electron transport in the NC monolayer can be described by (assuming ohmic conduction and Gerischer model for electron-transfer kinetics)<sup>6</sup>

$$\frac{\partial^2 \tilde{\mu}}{\partial R^2} + \frac{1}{R} \frac{\partial \tilde{\mu}}{\partial R} - \frac{K^0}{\Sigma} ((1 - C)e^{\tilde{\mu}/2} - Ce^{-\tilde{\mu}/2}) = 0 \quad (1)$$

where  $\tilde{\mu} = (\mu - \mu^0)/k_B T$  is the dimensionless electrochemical potential of the electrons in the NC monolayer,  $K^0 = k^0 r_e / D$  is the dimensionless standard rate constant of the electron-transfer reaction between the solution redox couple and the nanoparticle film ( $r_e$  is the electrode radius and  $D$  the redox mediator diffusion coefficient),  $C$  the dimensionless concentration of the solution redox couple at the substrate, and  $\Sigma$  the dimensionless conductivity in the film given by  $\Sigma = \sigma k_B T \Delta z / (e^2 r_e D c^b N_A)$ , where  $\sigma$  is conductivity,  $\Delta z$  the thickness of the film (taken as the diameter of the particles), and other symbols have their usual meaning. The electrochemical potential of the electrons in the NC film reaches an equilibrium value,  $\tilde{\mu}_{\text{eq}}$ , outside the tip–substrate gap. This is determined by the concentration ratio of the oxidized and reduced forms of the redox couple. SECM feedback response is governed by  $\Sigma$  and  $K^0$ : for fast kinetics, approach curves between the extremes of pure negative and positive feedback can be obtained.<sup>6</sup> This is due to the interplay between the diffusion flux of the solution redox mediator and the electron flux in the monolayer; at high redox couple concentrations, negative feedback due to hindered diffusion to the SECM tip is observed. Note that  $\Sigma$  is a function of both  $\sigma$  and  $c^b$ ; to experimentally observe negative feedback with realistic concen-

<sup>†</sup> University of Utrecht.

<sup>‡</sup> Helsinki University of Technology.

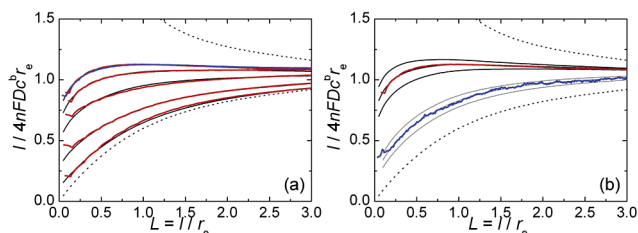


**Figure 2.** (a) Range of experimental approach curves where normalized tip current is plotted as a function of the normalized distance to the NC film ( $\text{Fe}(\text{CN})_6^{4-}$  concentrations from top to bottom: 0.03 (blue) and 0.13, 0.32, 0.66, 1.7, 7.0 mM (red) and the corresponding fits to the theory with  $K^0 = 0.2$  (black). The deposition surface pressure of the NC monolayer was  $20 \text{ mN m}^{-1}$ . (b) Experimental approach curves at film deposition surface pressure of  $3 \text{ mN m}^{-1}$  (blue) or  $20 \text{ mN m}^{-1}$  (red) with  $\text{Fe}(\text{CN})_6^{4-}$  concentration of  $1.1 \mu\text{M}$  and  $0.13 \text{ mM}$ , respectively. Theoretical approach curves for  $\Sigma = 2.5$  with  $K^0 = 0.25, 0.2$ , and  $0.15$  (black, top to bottom) and  $\Sigma = 3.6$  with  $K^0 = 0.04, 0.03$ , and  $0.02$  (gray, top to bottom).  $\bar{\mu}_{\text{eq}} = 3.17$  ( $E_{\text{eq}} = -82 \text{ mV}$  wrt  $E^\circ$ ). The dashed lines are the theoretical response for pure positive and negative feedback.

trations,  $\sigma$  values must be low. As the concentration is reduced, the relative contribution of mediator regeneration due to lateral electron transport in the film increases and at sufficiently low concentrations, pure positive feedback should be reached. Under kinetic control, pure positive feedback will not be observed for any finite value of  $\Sigma$  (for a given value of  $\bar{\mu}_{\text{eq}}$ ), the feedback saturates at a value determined by  $K^0$  (Supporting Information).

A series of approach curves to the NC film in the metallic state with different concentration of  $\text{Fe}(\text{CN})_6^{4-}$  are shown Figure 2a. It can be seen that the observed feedback saturates as the mediator concentration is lowered. At the lowest concentrations, the feedback response is governed solely by the ET rate. The experimental approach curves were fitted to the theory with  $K^0 = 0.2$  (Figure 2a, black lines). The sensitivity of the fitting to the kinetic parameter  $K^0$  is demonstrated in Figure 2b.

The monolayer conductivity determined ( $0.018 \Omega^{-1} \text{ cm}^{-1}$ ) is inline with that obtained previously with ferrocene methanol (FcMeOH) as the redox mediator (Supporting Information) where kinetic limitations were not noted. This clearly demonstrates that the relative contributions of ET kinetics and conductivity to the feedback response can be fully separated. The  $k^0$  value determined,  $(1.1 \pm 0.2) \times 10^{-3} \text{ cm s}^{-1}$ , is 4 orders of magnitude higher than that predicted based on the known distance dependence of tunneling through a monolayer.<sup>2</sup> Taking the rate constant at a bare Au electrode to be  $0.03 \text{ cm s}^{-1}$ , the rate can be estimated as  $k_{\text{Au}} \exp(-\beta d) \approx 1.8 \times 10^{-7} \text{ cm s}^{-1}$  (with  $\beta = 1/\text{methyl unit}$ ).<sup>2c,f</sup> The difference between the experimental and predicted rates could be ascribed to the redox molecule being able to approach the Au core more closely due to the less ordered nature of the SAMs formed on the surface of nanoparticles.<sup>2d,3c</sup> Due to the high radius of curvature, there is a decrease in chain density moving away from the surface of the core.<sup>3</sup> However, for particles of the size used here, this effect is believed to be less pronounced as the majority of the surface comprises of flat (111) facets rather than edges and corners.<sup>7</sup> This geometry leads to bundles of ordered alkanethiolates on the terraces with gaps at the corners and vertexes.<sup>7</sup> These gaps can be considered as defects where ET is not blocked leading to observed higher rates.<sup>2d</sup>

Approach curves obtained for the insulating film are given in Figure 2b and Supporting Information. The experimental feedback response also saturates at low mediator concentrations where only kinetics control the observed response. Due to the exceedingly low concentrations needed to reach this regime, it is difficult to

independently fit both the film conductivity and the kinetics. Hence, we used the value of the conductivity determined with FcMeOH as the redox species ( $2 \times 10^{-4} \Omega^{-1} \text{ cm}^{-1}$ ).<sup>6</sup> As can be seen in Figure 2b, the level of feedback is lower than with a monolayer deposited at  $20 \text{ mN m}^{-1}$  (despite higher  $\Sigma$ ). This indicates that the kinetics of electron transfer between the solution redox couple and the NC film depends on the state of the monolayer. The experimental curves fit well to theory with  $K^0 = 0.03$  corresponding to  $k^0 = (1.7 \pm 0.5) \times 10^{-4} \text{ cm s}^{-1}$  (Supporting Information). This is an order of magnitude lower than that determined for the metallic film. This difference is not due to the smaller number of NCs available under the SECM tip at low surface pressure as the NC mean molecular area changes by less than 30%. The observed dependence of the ET rate can be rationalized in terms of the charging energy.<sup>5</sup> For the metallic film, electrons are delocalized over several NCs and the charging energy associated with removing/adding an electron is negligible. In contrast when the film is insulating, the charging energy to inject an additional electron (hole) to an individual nanocrystal must be overcome. The presence of this extra energy barrier decreases the rate of electron transfer to the metal core.

In summary, we have demonstrated that the rate of electron transfer across dodecanethiol SAM on a gold nanocrystal is several orders of magnitude higher than on a macroscopic Au electrode. There is a profound difference in the rate of ET depending on the redox couple used (FcMeOH vs  $\text{Fe}(\text{CN})_6^{4-}$ ), illustrating the importance of molecule specific properties, such as the effect of their relative hydrophilicities. In addition, the effect of Coulomb blockade on electrochemical kinetics was observed. As film conductivity and kinetic parameters can be independently determined, this approach offers a route to study the individual and collective properties of functionalized nanoparticles.

**Acknowledgment.** This research was funded by the Academy of Finland and the EU (“NANOSPECTRA”, HPRH-CT-2001-00320). We are grateful to Daniël Vanmaekelbergh and John Kelly for their comments.

**Supporting Information Available:** Additional details on the SECM model and experimental results. This material is available free of charge via the Internet at <http://pubs.acs.org>.

## References

- (1) (a) Adams, D. M.; et al. *J. Phys. Chem. B* **2003**, *107*, 6668. (b) Gray, H. B.; Winkler, J. R. *Proc. Nat. Acad. Sci.* **2005**, *102*, 3534. (c) Nitzan, A.; Ratner, M. A. *Science* **2003**, *300*, 1384.
- (2) (a) Chidsey, C. E. D. *Science* **1991**, *251*, 919. (b) Slowinski, K.; Chamberlain, R. V.; Miller, C. J.; Majda, M. *J. Am. Chem. Soc.* **1997**, *119*, 11910. (c) Liu, B.; Bard, A. J.; Mirkin, M. V.; Creager, S. E. *J. Am. Chem. Soc.* **2004**, *126*, 1485. (d) Slowinski, K.; Slowinska, K. U.; Majda, M. *J. Phys. Chem. B* **1999**, *103*, 8544. (e) Terretaz, S.; Becka, A. M.; Traub, M. J.; Fetting, J. C.; Miller, C. J. *J. Phys. Chem.* **1995**, *99*, 11216. (f) Khoshtariya, D.; Dolidze, T. D.; Zusan, L. D.; Waldeck, D. H. *J. Phys. Chem. A* **2001**, *105*, 1818.
- (3) (a) Love, J. C.; Estroff, L. A.; Kriebel, J. K.; Nuzzo, R. G.; Whitesides, G. M. *Chem. Rev.* **2005**, *105*, 1103. (b) Daniel, M.-C.; Astruc, D. *Chem. Rev.* **2004**, *104*, 293. (c) Templeton, A. C.; Wuelfing, W. P.; Murray, R. W. *Acc. Chem. Res.* **2000**, *33*, 27.
- (4) (a) Wuelfing, W. P.; Green, S. J.; Pietron, J. J.; Cliffel, D. E.; Murray, R. W. *J. Am. Chem. Soc.* **2000**, *122*, 11465. (b) Brennan, J. L.; Branham, M. R.; Hicks, J. F.; Osisek, A. J.; Donkers, R. L.; Georganopoulou, D. G.; Murray, R. W. *Anal. Chem.* **2005**, *76*, 5611.
- (5) Markovich, G.; Collier, C. P.; Henrichs, S. E.; Remacle, F.; Levine, R. D.; Heath, J. R. *Acc. Chem. Res.* **1999**, *32*, 415.
- (6) Liljeroth, P.; Vanmaekelbergh, D.; Ruiz, R.; Kontturi, K.; Jiang, H.; Kauppinen, E.; Quinn, B. M. *J. Am. Chem. Soc.* **2004**, *126*, 7126.
- (7) Wang, Z. L.; Harfenist, S. A.; Whetten, R. L.; Bentley, J.; Evans, N. D. *J. Phys. Chem. B* **1998**, *102*, 3068.

JA057474O